Aesth Plast Surg (2015) 39:134–140
DOI 10.1007/s00266-014-0418-z

ORIGINAL ARTICLE EXPERIMENTAL/SPECIAL TOPICS

The Inhibitory Effect of Platelet-Rich Plasma on Botulinum Toxin Type-A: An Experimental Study in Rabbits

Hakan Bulam · Suhan Ayhan · Billur Sezgin · Murat Zinnuroglu · Ece Konac · Nuray Varol · Kemal Findikcioglu · Serhan Tuncer · Seyhan Cenetoglu

Received: 16 July 2014 / Accepted: 16 October 2014 / Published online: 21 November 2014

Abstract

Background Combination treatments of botulinum toxin type-A and other rejuvenation agents or instruments are gradually becoming more popular. After observing a high incidence of therapy failure following simultaneous applications of botulinum toxin type-A and platelet-rich plasma mesotherapy, we aimed to investigate whether PRP has an inhibitory effect on botulinum toxin type-A.

Methods Twenty-four New Zealand white rabbits were divided into 4 groups, and the anterior auricular muscle and overlying skin were used for injections. Groups I and II both received onabotulinumtoxinA intramuscular injections. In addition, autologous platelet-rich plasma mesotherapy was performed in Group I while Group II received saline mesotherapy. Group III was designed as the in vitro mixture group in which onabotulinumtoxinA and platelet-rich plasma were mixed and then administered intramuscularly. Group IV received saline within the mixture instead of platelet-rich plasma. The contralateral ears of all the rabbits served as control and were only treated with onabotulinumtoxinA. Visual evaluation of ear positions and electroneuromyographic studies were done prior to all procedures and at day 14. Anterior auricular muscles were harvested at day 14 and were evaluated with quantitative real-time PCR.

Results Visual and electroneuromyographic studies revealed less onabotulinumtoxinA activity in Groups I and III. When platelet-rich plasma was administered through skin mesotherapy, onabotulinumtoxinA activity failure was more severe in comparison with direct contact. No significant difference in SNAP-25 mRNA expression through quantitative real-time PCR was observed between groups.

Conclusion Although we could not explain the exact mechanism underlying this interaction, platelet-rich plasma applications result in less onabotulinumtoxinA muscle paralysis activity.

No Level Assigned This journal requires that authors assign a level of evidence to each submission to which Evidence-Based Medicine rankings are applicable. This excludes Review Articles, Book Reviews, and manuscripts that concern Basic Science, Animal Studies, Cadaver Studies, and Experimental Studies. For a full description of these Evidence-Based Medicine ratings, please refer to the Table of Contents or the online Instructions to Authors http://www.springer.com/00266.

Keywords Botulinum toxin type-A · Inhibitors · Metalloproteases · Platelet-rich plasma · SNAP-25 protein

This study was presented at the 2nd European Association of Plastic Surgeons Research Council Meeting, Antalya, Turkey, 22–23 May 2013 and was awarded second place in the "Scientific Competition of Residents-Experimental Studies" at the 35th Congress of the Turkish Society of Plastic Reconstructive and Aesthetic Surgery, October 28–31, 2013 Istanbul, Turkey.

H. Bulam · S. Ayhan (✉) · B. Sezgin · K. Findikcioglu · S. Tuncer · S. Cenetoglu
Department of Plastic Reconstructive and Aesthetic Surgery, Gazi University Faculty of Medicine, Ankara, Turkey
e-mail: suayhan@gmail.com

M. Zinnuroglu
Department of Physical Therapy and Rehabilitation, Gazi University Faculty of Medicine, Ankara, Turkey

E. Konac · N. Varol
Department of Medical Biology and Genetics, Gazi University Faculty of Medicine, Ankara, Turkey

Introduction

More than six million botulinum toxin type-A (BoNT-A) applications were reported in the United States during the year 2013 [1]. In recent years, combination therapies of BoNT-A applications together with injectable fillers, mesotherapy agents, chemical peeling agents, radiofrequency, and lasers have been widely performed to reach more favorable results in facial rejuvenation. Among these, platelet-rich plasma (PRP) mesotherapy particularly has the advantage of stimulating proliferation and angiogenesis. The contribution of PRP to cell proliferation is thought to be based on the growth factors (PDGF, VEGF, TGF-β, EGF, and IGF-1) present within it [2].With technical innovations in preparation and increased availability, the frequency of PRP mesotherapy procedures has gradually increased.

The mechanism of botulinum toxin has four critical stages: binding to presynaptic membranes, internalization with endocytosis, translocation to the cytoplasm, and proteolysis of SNARE (soluble *N*-ethylmaleimide attachment protein receptor) proteins. By breaking the SNAP-25 (synaptosome-associated protein of 25 kDa) protein with the zinc-metalloproteinase activity of its light chain, BoNT-A prevents acetylcholine release to the neuromuscular junction. To achieve the muscle paralysis effect, all stages must be accomplished. Therapeutic failure of BoNT-A in cosmetic use is very uncommon [3]. Although it has yet to be proven, in most cases, it has generally been assumed that the reason for therapeutic failure was the neutralizing antibodies against the BoNT-A.

Platelets consist of three different types of granules, and following degranulation, plenty of molecules, growth factors, coagulation factors, and enzymes are released into the medium. The therapeutic effects of PRP regarding growth factors are known but the effect of the others enzymes and molecules are still under assessment.

In our practice, we encountered therapeutic failure or a shorter duration of muscle paralysis following BoNT-A injections, only in such cases where PRP mesotherapy was performed at the same session. This experimental study was designed following this clinical observation, and the purpose was to investigate whether PRP has an inhibitory effect on BoNT-A.

Materials and Methods

The study was approved by the Institutional Ethics Committee for Animal Studies. The study was carried out on 24 male New Zealand white rabbits weighing between 1.5 and 2 kg. For surgical procedures, rabbits were anesthetized with an anesthetic cocktail consisting of ketamine (1.5 mL, 100 mg/mL), acepromazine (0.5 mL, 10 mg/mL), and xylazine (0.5 mL, 20 mg/mL). Each animal received 0.5 mL/kg of the anesthetic cocktail intramuscularly. The periauricular area and inguinal area were shaved before electroneuromyographic studies, blood sampling, and each injection.

The anterior auricular muscle model was selected for the study, since it was a suitable model for visual, electroneuromyographic, and muscle biopsy evaluations. As a pilot study, an anatomical dissection of the anterior auricular muscle was performed in a rabbit cadaver, and anatomical details of the muscle were recorded. The anterior auricular muscle origin was located at the frontal bone, about 2 cm cranial to the medial canthus, and it inserted along the ventromedial border of the ipsilateral ear, about 3 cm from the base of the ear. Injection points and set-up of electrodes were designed on the basis of these anatomical details.

OnabotulinumtoxinA (Botulinum toxin type-A, Botox®; Allergan, Abdi Ibrahim, Turkey) was used for botulinum toxin injections following reconstitution with 2 mL of sterile saline. In the present study, we used 2.5 U (0.05 mL) BoNT-A for botulinum toxin injections.

Autogenous PRP was prepared for each rabbit. Ten cc blood samples were obtained through the inguinal artery. The Regen-ACR (Regenlab, Switzerland) PRP preparation kit was used to obtain PRP. Blood was processed according to the recommended protocol of the PRP kit. The blood was administered to the kit's tube, and the tube was centrifuged at 3100 rpm/min for 8 min with the JK-LC-802C (Jingke, China) centrifuge. One cc of PRP was obtained at the end of the procedure.

All BoNT-A and PRP injections were performed by the same researcher and the same technique. Botulinum toxin was injected intramuscularly to the middle of the muscle belly, and PRP was injected subcutaneously through multiple and small volume punctures to simulate the mesotherapy procedure. Thirty-gage syringes were used for all types of injections.

The animals were divided into four groups:

Group I (PRP Mesotherapy Group) ($n = 6$): Animals received an injection of 2.5 U (0.05 mL) BoNT-A into both right and left anterior auricular muscles. The 2 × 1 cm sized skin overlying the right anterior auricular muscle was treated with 1 mL PRP intradermally by multiple serial small volume punctures.

Group II (Mesotherapy Group) ($n = 6$): Animals received an injection of 2.5 U (0.05 mL) BoNT-A into both right and left anterior auricular muscles. The 2 × 1 cm sized skin overlying the right anterior auricular muscle was treated with 1 mL %0.9 NaCl intradermally by multiple serial small volume punctures.

Fig. 1 Grading system for the rabbit auricle. All *left* ears completely dropped following the BoNT-A injection. Grading was performed according to level of *right* ears. Grade 1: Completely paralytic *right* ear, dropping more than 60° (high paralytic activity of BoNT-A). Grade 2: Moderately paralytic *right* ear, dropping between 30° and 60° (moderate paralytic activity of BoNT-A). Grade 3: Mildly paralytic *right* ear, *right* ear can rise more than 60° (low paralytic activity of BoNT-A)

Group III (PRP and BoNT-A in vivo mixture Group) ($n = 6$): Animals received an injection of 2.5 U (0.05 mL) BoNT-A plus 0.05 mL PRP into the right anterior auricular muscles and 2.5 U (0.05 mL) BoNT-A into the left anterior auricular muscles.

Group IV (Control in vivo mixture Group) ($n = 6$): Animals received an injection of 2.5 U (0.05 mL) BoNT-A plus 0.05 mL NaCl into the right anterior auricular muscles and 2.5 U (0.05 mL) BoNT-A into the left anterior auricular muscles.

Following visual and electroneuromyographic studies, the anterior auricular muscles were excised bilaterally through a bitemporal incision on post-injection day 14 and were processed by quantitative real-time PCR analysis.

Visual Evaluation

All rabbits had healthy, mobile ears in upright positions before the injections. With the effect of the BoNT-A, the action of the anterior auricular muscle was paralyzed and ears dropped. The ear positions of the rabbits were evaluated blindly on day 14 after the injections and were graded with a three-grade evaluation system (Fig. 1). Dropping of more than 60° was observed in the left ear of all rabbits, and left ears were used as controls. This finding showed that the dose of injected BoNT-A was sufficient to paralyze the anterior auricular muscles. The positions of the right ears were used as indicators of efficiency of the BoNT-A. Grade 1 indicated high BoNT-A activity, Grade 2 moderate, and Grade 3 low BoNT activity.

Electroneuromyographic Studies

The Medelec Synergy EMG system (VIASYS HealthCare, UK) was used for the electroneuromyographic studies. All assessments were performed in standard motor nerve conduction settings [low-frequency filter, 2 Hz; high-frequency filter, 10 kHz; stimulus intensity was increased in a stepwise manner until a supramaximal motor response was elicited (usually between 5 and 50 mA), and stimulus duration was 0.2 ms]. Three surface disk electrodes were used to measure the compound muscle action potential. Before the study, the anatomical dissection of the anterior auricular muscle was done in a rabbit cadaver (Fig. 2). The anterior auricular muscle originated from the frontal bone, about 2 cm cranial to the medial canthus, and inserted along the ventromedial border of the ipsilateral ear, about 3 cm from the base of the ear. The electrodes were placed considering the muscle belly and tendon principle. The active recording electrode was placed at the center (muscle belly) of the anterior auricular muscle, the reference recording was placed at the insertion (tendon), and the ground electrode was placed on the posterior surface of the ear. These three locations were marked with a permanent marker and used for repeated measurements. A supramaximal stimulation was given to the rostral branches of

Fig. 2 Anatomical dissection of the anterior auricular muscle. The origin of the muscle is indicated with *white arrows*, and the insertion is indicated as *black arrow*. The intramuscular injection is also demonstrated

the facial nerve which was stimulated through the overlying masseter muscle at the cheek between the lower eyelid and jaw at lateral decubitus position for the stimulation of the motor nerve of the anterior auricular muscle.

Compound muscle action potentials (CMAP) were recorded by supramaximal stimulation of the facial nerve, and the amplitude of the elicited CMAPs was measured. This procedure was repeated three times, and one of the three CMAPs which had the maximum amplitude value was used for statistical evaluation.

Total RNA Extraction and cDNA Preparation

Total RNA was extracted using Tripure Reagent (Roche, Invitrogen, Darmstadt, Germany) according to the manufacturer's protocol. To avoid DNA contamination, we performed some modifications to the manufacturer's instructions. Tissues were homogenized and incubated in Trizol (100 mg/mL Trizol) for 5 min, and the RNA was separated using chloroform (0.2 mL/1 mL Trizol). After centrifugation at 12,000*g* for 15 min at 4 °C, the aqueous phase of the sample was transferred to a fresh tube for RNA precipitation by isopropyl alcohol (0.5 mL/1 mL Trizol). After repeating incubation and centrifugation as above, the pellet was washed with 75 % ethanol. The mixture was centrifuged at 7500*g* for 5 min at 4 °C. Finally, the air-dried pellet was re-dissolved with DEPC-treated water. The yield and quality of the RNA of each sample were determined by measuring the absorbance at 260 and 280 nm using the "Nano Drop Spectrophotometer" (NanoDrop ND-1000, Montchanin, DE, USA). The ratio of sample absorbance $A_{260/280} < 2.0$ and $A_{260/230}$ in the range of 1.8–2.2 was considered an acceptable measure of RNA purity. Total RNA (1 μg) was reverse-transcribed in a 20 μL reaction mixture using random hexamers and a Transcriptor First Strand cDNA synthesis kit (Roche Diagnostics GmbH, Mannheim, Germany) according to the manufacturer's instructions.

Quantitative Real-Time PCR (QRT-PCR) Analysis

SNAP25 mRNA expression levels were measured using the real-time PCR method. Probe and primer sets for SNAP25 gene were designed at the Universal Probe Library Assay Design Center (URL: www.roche-applied-science.com and UPL probe number for SNAP25 was 58). Primers used in this section were shown as follows: SNAP25: 5′-AAA AAG CCT GGG GCA ATA AT-3′ (forward primer), 5′-CTT TCG TCC ACC ACA CGA G-3′ (reverse primer); HPRT: 5′-GCT TTC CTT GGT CAA GCA GT-3′ (forward primer), 5′-CAC TTC GAG GGG TCC TTT TC-3′ (reverse primer). The 10 μL reaction mixture prepared in a LightCycler ® 480 Multiwell Plate 96 contained LightCycler® 480 Probes Master reaction mixture (Roche Diagnostics, GmbH, Mannheim, Germany), 2.5 pmol of each primer, 1 pmol of UPL probe, 4 mM $MgCl_2$, and 1 μL cDNA. The real-time PCR assay included a no-template control. All PCR reactions were performed in the LightCycler ® 480 instrument (Roche Diagnostics, GmbH, Mannheim, Germany) using the following program conditions: 95 °C for 10 min followed by 45 cycles at 95 °C for 10 s, 60 °C for 20 s, and finally a cooling step to 40 °C. We analyzed the expression of the HPRT housekeeping gene to normalize the results obtained by QRT-PCR. Each sample was tested in triplicate. PCR efficiency for each gene was tested by serial dilutions, and amplification efficiencies of target gene and HPRT for each gene were approximately equal.

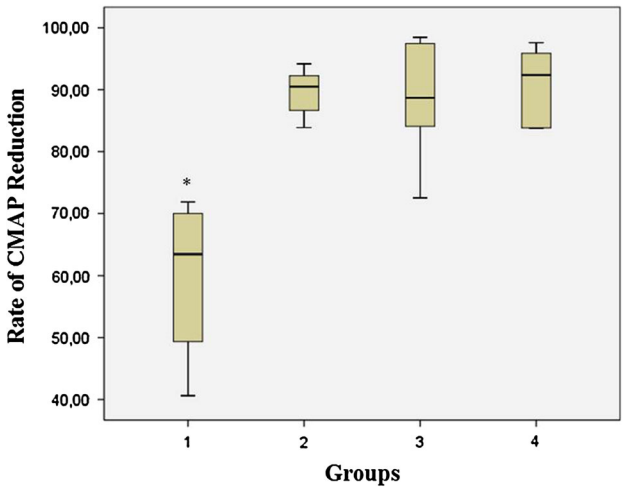

Fig. 3 Rate of CMAP Reduction in *right* ears. CAMP reduction was significantly lower in the PRP mesotherapy-treated group than other groups. (*$P < 0.05$)

Statistical Analysis

Data of visual and electroneuromyographic studies were analyzed by the Chi-square test, Wilcoxon signed test, and Kruskal–Wallis tests, using SPSS 11.0 for Windows. Statistical significance levels of differences in mRNA expressions were analyzed by pair-wise fixed reallocation randomization test. The REST software Tool 2009 version 2.013 was used for group-wise comparison and statistical analysis of relative expression results [4]. $P < 0.05$ (Mann–Whitney *U* test) was considered statistically significant. The results were expressed in form of mean ± SD.

Table 1 Electroneuromyographic results 24 h after injection

Groups	Subjects	Compound muscle action potentials (CMAP) (mV)			
		R^0	R^{14}	L^0	L^{14}
Group I	N1	19.9	5.6	15.7	1.3
	N2	15.6	7.9	12.5	4.6
	N3	7.24	4.3	13.4	0.2
	N4	19.0	5.7	14.3	1.1
	N5	12.2	4.8	19.1	4.0
	N6	8.9	3.0	14.4	0.9
P	0.028				
Group II	N1	10.3	0.6	11.8	1.2
	N2	12.2	1.1	11.3	1.2
	N3	9.0	1.2	16.6	1.0
	N4	9.0	0.9	10.4	0.8
	N5	12.9	1.0	9.6	0.8
	N6	9.3	1.5	11.5	1.5
P	0.60				
Group III	N1	9.1	2.5	9.5	1.2
	N2	13.8	1.4	14.6	0.8
	N3	12.9	0.2	14.7	0.1
	N4	11.8	0.3	11.9	0.3
	N5	9.6	1.2	8.8	0.7
	N6	8.8	1.4	11.3	0.5
P	0.038				
Group IV	N1	11.7	0.9	11.9	0.8
	N2	13.6	2.2	13.5	2.1
	N3	12.5	0.3	12.2	0.3
	N4	7.4	1.2	5.6	0.4
	N5	9.7	0.4	12.7	0.8
	N6	6.6	0.5	8.7	1.2
P	0.91				

R^0 Right ear anterior auricular muscle compound muscle action potential (CMAP) before injections, R^{14} Right ear anterior auricular CMAP 14 days after injections, L^0 Left ear anterior auricular CMAP before injections, L^{14} Left ear anterior auricular muscle CMAP 14 days after injections

Results

According to visual evaluation studies, 83 % of the rabbits in Group I were classified as Grade 2 and Grade 3 ears (Fig. 3). In the groups II, III, and IV, the number of the subjects with Grade 2 and Grade 3 ears was 17, 33, and 17 %, respectively. When compared with the other groups, right ears of the rabbits in Group 1 were in a significantly higher position ($P < 0.05$).

According to the results of the electroneuromyographic studies, muscle action potential amplitudes at day 14 were significantly higher compared to the contralateral side measurements in Group I and Group III (Table 1). The rates of decrease in the amplitude of the compound muscle action potential (CMAP) were calculated with the formulation of

$$\text{Rate of CMAP amplitude decrease} = \frac{\text{CMAP0} - \text{CMAP14}}{\text{CMAP0}} \times 100$$

(CMAP0: CMAP before injections, CMAP14: 14 days after injections)

As seen in Fig. 3, the mean CMAP amplitude reduction rates in the right ears of Group 1 were significantly lower than other groups ($P = 0.004$). No significant difference was found regarding the left ears in the subjects of all groups.

When we compared the left ear anterior auricular muscle groups with the right ear groups, we found no significant difference in the mRNA expression levels of the *SNAP25* gene (Fig. 4).

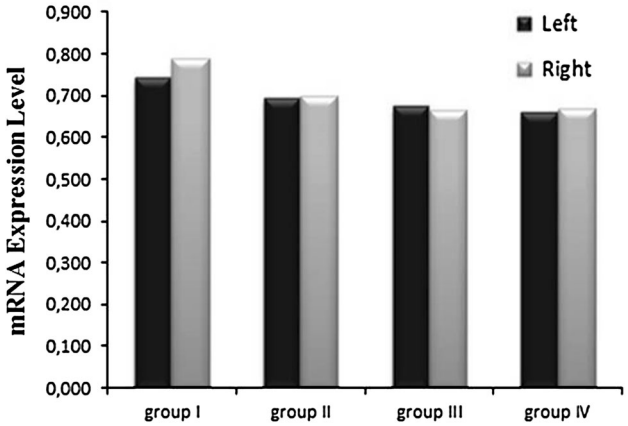

Fig. 4 mRNA expression levels of the SNAP25 gene in the *left* and *right* ear anterior auricular muscles of all groups (G1, G2, G3, and G4)

Discussion

PRP applications have been performed in various areas and different specialties of medicine especially for wound, bone, nerve and joint cartilage healing, skin rejuvenation, and fat graft survival [5–8]. Despite more recent clinical use, the proliferative effect of PRP was shown by Kim et al. in 2011 [9]. They stated that PRP has a proliferative effect on fibroblasts, which leads to an increase in type-1 collagen expression. However, the efficiency and reliability of mesotherapy applications are controversial [10, 11].Taieb et al. reported high patient satisfaction three months after hyaluronic acid and mannitol mesotherapy [12]. Similarly, Lacarrubbba et al. found that hyaluronic acid mesotherapy can positively affect the skin photo-aging

process [13]. However, there are also contrary results in some other studies. El-Domyati et al. stated that no significant changes in skin were detected in clinical and histopathological evaluations following mesotherapy sessions [14]. Amin et al. reported ineffective results of hyaluronic acid mesotherapy for skin rejuvenation [15].

Although mesotherapy is a cutaneous procedure, theoretically injected drugs or molecules have the potential to reach deeper structures such as muscles or joints. Therefore, mixtures of piroxicam, ketorolac, baclofen, diazepam, buflomedil, and pentoxifylline have been used through the mesotherapy route as a treatment option in osteoarthritis, fibromyalgia, tendinitis, bursitis, and back pain [16]. So theoretically intradermal injections of PRP can impact underlying tissues or muscles. Therefore, intramuscular botulinum toxin injections and intracutaneous PRP therapy are able to interact in a combined skin rejuvenation session.

Platelets have three different types of granules: alpha, delta, and lambda granules. The alpha granules consist of coagulation factors, growth factors, glycoproteins (fibronectin, vWF), proteoglycans, albumin, immunoglobulins, and protease inhibitors (alpha-2 macroglobulin and alpha-2 antiplasmin). The content of the granules spreads to the surrounding media when platelets are activated by matrix components (collagen, laminin, and fibronectin), hormones (epinephrine and vasopressin), thrombin, thromboxane A2, and calcium. The primary role of alpha-2 macroglobulin and alpha-2 antiplasmin is inhibition of fibrinolysis through the inhibition of plasmin. Beside this major function, alpha-2 macroglobulin is also known as a general protease inhibitor and has an inhibitory effect on serine, cysteine, treonin, and aspartic proteases as well as metalloprotease [17]. When we consider that the active light chain portion of the BoNT-A has zinc metalloprotease activity on the SNAP-25 protein, theoretically we can speculate that this enzymatic interaction is a possible explanation for the inhibitory effect of PRP on BoNT-A. There are few studies about the inhibitory effect of alpha-2 macroglobulin on different toxins. *Vibrio vulnificus*, an opportunistic human pathogen, produces a 45-kDa zinc metalloprotease and causes a typical hemorrhagic skin lesion. Miyoshi et al. found that the toxin of *V. vulnificus* can be quickly inactivated by alpha-2 macroglobulin [18]. In another study, Saidi et al. stated that alpha-2 macroglobulin could interact with snake venom called lebetase and inhibit its fibrinolytic metalloprotease activity [19].

PRP has been shown to enhance nerve healing due to its growth factor content. Especially IGF, VEGF, TGF-β, PDGF, and FGF- II play important roles in nerve regeneration by stimulation of axonal outgrowth and Schwann cell proliferation and protein and lipid synthesis, which are necessary for nerve regeneration [8, 20, 21]. The action of BoNT-A ends by axonal sprouting, formation of new neuromuscular junctions, and recovery of the affected neuromuscular junctions. Therefore, the growth factor content of PRP may also interact with this regeneration process and may lead to a decrease in the duration of BoNT-A activity. A long-term study will be more appropriate to evaluate this effect of PRP on BoNT-A activity.

The anterior auricular muscle model was first introduced by Jabor et al. in 2003 [22].They compared efficiency of freshly reconstituted and stored botulinum toxin. Before the main study, they conducted a pilot study to determine the BoNT-A dose for paralysis of the anterior auricular muscle. They found that 2.5 U BoNT-A was the safest minimum dose that could yield complete paralysis of the muscle. This model has also been used in several studies after the initial study, yielding the advantages to perform visual, electroneuromyographic, and muscle biopsy-based studies [23, 24].

Toxin inhibitors target a variety of intoxication steps. Binding, internalization, translocation, and enzymatic toxicity have been targets of candidate botulinum toxin inhibitors. Antibody-based treatments have been known as the only antitoxin option until the early 2000 s. They can inactivate the toxin in circulation but the circulation interval of the toxin is very short, and once the toxin is bound to the nerve terminal, antibodies were ineffective. The toxic reaction step involving the Zn-metalloprotease activity on one of the SNARE proteins has been the major focus of attention over the last decade. The first irreversible inhibitor, based on the benzylidenecyclopentenedione structure that leads to covalent modification of the active site of botulinum toxin type-A, was discovered by Capcova et al. in 2010 [25]. But still there are two important handicaps that need to be solved in the production of a botulinum antitoxin. One of these is the toxicity of the antitoxin itself and different level efficacies of the antitoxins in in vivo and cellular-based mediums. Toxicity and efficacy studies regarding botulinum antitoxin are still ongoing.

Botulinum toxin injections can cause unintended local side effects either from technical errors or from diffusion of the botulinum toxin to muscles other than the targeted. Overdose treatments can more likely result in lid ptosis, ectropion, strabismus, lip dysfunction, dysphagia, brow malposition, or mask-face depending on the injection area [26]. Solutions for accidental overdose BoNT-A treatments are generally based on symptomatic treatments and they aim to gain time until the effects of the injection decrease. In our opinion, PRP can be used as an autologous and easily accessible option for the treatment of botulinum toxin overdose.

SNAP-25 mRNA expression was observed in all muscle samples. No significant difference was found between groups and the right/left side anterior auricular muscles of rabbits. It can be assumed that maybe there was a

difference in post-transcriptional or translational modification levels.

Conclusion

In conclusion, it seems that PRP has an inhibitory effect on BoNT-A, when applied simultaneously. We suggest performing these two applications in separate sessions. We could not define the exact mechanism behind the inhibitory effect but alpha-2 macroglobulin may lead to this interaction between BoNT-A and PRP. More detailed molecular studies can explain the mechanism of interaction and whether PRP can decrease the duration of effect once the paralytic effect of botulinum toxin is totally achieved.

Acknowledgments This study was approved by the Gazi University Ethical Committee for Experimental Research on Animals (Project no: G.U. ET-43-6865) and was financially supported by the Gazi University Research Fund (Project no: 01/2012-60).

Conflict of interest The authors declare that they have no conflicts of interest to disclose within the blinded manuscript.

Statement of Animal Rights All applicable institutional and/or national guidelines for the care and use of animals were followed.

References

1. American Society of Plastic Surgeons 2013 Plastic Surgery Statistics Report. http://www.plasticsurgery.org/Documents/news-resources/statistics/2013-statistics/cosmetic-procedures-national-trends-2013.pdf
2. Man D, Plosker H, Winland-Brown JE (2001) The use of autologous platelet-rich plasma (platelet gel) and autologous platelet-poor plasma (fibrin glue) in cosmetic surgery. Plast Reconstr Surg 107(1):229–237
3. Naumann M, Carruthers A, Carruthers J et al (2010) Meta-analysis of neutralizing antibody conversion with BoNT-A (BOTOX®) across multiple indications. Mov Disord 25(13):2211–2218
4. Pfaffl MW, Horgan GW, Dempfle L (2002) Relative expression software tool (REST) for group wise comparison and statistical analysis of relative expression results in real-time PCR. Nucleic Acids Res 30:e36
5. Findikcioglu K, Findikcioglu F, Yavuzer R, Elmas C, Atabay K (2009) Effect of platelet-rich plasma and fibrin glue on healing of critical-size calvarial bone defects. J Craniofac Surg 20(1):34–40
6. Cho JM, Lee YH, Baek RM, Lee SW (2011) Effect of platelet-rich plasma on ultraviolet b-induced skin wrinkles in nude mice. J Plast Reconstr Aesthet Surg 64(2):e31–e39
7. Cervelli V, Palla L, Pascali M, De Angelis B, Curcio BC, Gentile P (2009) Autologous platelet-rich plasma mixed with purified fat graft in aesthetic plastic surgery. Aesthetic Plast Surg 33(5):716–721
8. Sariguney Y, Yavuzer R, Elmas C, Yenicesu I, Bolay H, Atabay K (2008) Effect of platelet-rich plasma on peripheral nerve regeneration. J Reconstr Microsurg 24(3):159–167
9. Kim DH, Je YJ, Kim CD, Lee YH, Seo YJ, Lee JH, Lee Y (2011) Can Platelet-rich Plasma Be Used for Skin Rejuvenation?. Evaluation of Effects of Platelet-rich Plasma on Human Dermal Fibroblast. Ann Dermatol 23(4):424–431
10. Bulam H, Ayhan S, Sezgin B, Özmen S, Çenetoğlu S (2013) Mesotherapy: is it a miracle or an air bubble on the tip of the needle? Turk Plast Surg 21(2):16–19
11. Rohrich RJ (2005) Mesotherapy: what is it? Does it work? Plast Reconstr Surg 115(5):1425
12. Taieb M, Gay C, Sebban S, Secnazi P (2012) Hyaluronic acid plus mannitol treatment for improved skin hydration and elasticity. J Cos-met Dermatol 11(2):87–92
13. Lacarrubba F, Tedeschi A, Nardone B, Micali G (2008) Mesotherapy for skin rejuvenation: assessment of the subepidermal low-echo genic band by ultrasound evaluation with cross-sectional B-mode scanning. Dermatol Ther 21(3):1–5
14. El-Domyati M, El-Ammawi TS, Moawad O et al (2012) Efficacy of mesotherapy in facial rejuvenation: a histological and immunohistochemical evaluation. Int J Dermatol 51(8):913–919
15. Amin SP, Phelps RG, Goldberg DJ (2006) Mesotherapy for facial skin rejuvenation: a clinical, histologic, and electron microscopic evaluation. Dermatol Surg 32(12):1467–1472
16. Herreros FO, Moraes AM, Velho PE (2011) Mesotherapy: a bibliographical review. An Bras Dermatol 86(1):96–101
17. Baker AH, Edwards DR, Murphy G (2002) Metalloproteinase inhibitors: biological actions and therapeutic opportunities. J Cell Sci 115(19):3719–3727
18. Miyoshi S, Shinoda S (1991) Alpha-macroglobulin-like plasma inactivator for Vibrio vulnificus metalloprotease. J Biochem 110(4):548–552
19. Saidi N, Samel M, Siigur J, Jensen PE (1999) Lebetase, an alpha (beta)-fibrin(ogen)olytic metalloproteinase of Viperalebetina snake venom, is inhibited by human alpha-macroglobulins. Biochim Biophys Acta 1434(1):94–102
20. Sjoberg J, Kanje M (1989) Insulin-like growth factor (IGF-1) as a stimulator of regeneration in the freeze-injured rat sciatic nerve. Brain Res 485:102–108
21. Sondell M, Lundborg G, Kanje M (1999) Vascular endothelial growth factor has neurotrophic activity and stimulates axonal outgrowth, enhancing cell survival and Schwann cell proliferation in the peripheral nervous system. J Neurosci 19:5731–5740
22. Jabor MA, Kaushik R, Shayani P, Ruiz-Razura A, Smith BK, Morimoto KW, Cohen BE (2003) Efficacy of reconstituted and stored botulinum toxin type A: an electrophysiologic and visual study in the auricular muscle of the rabbit. Plast Reconstr Surg 111(7):2419–2426
23. Elmas C, Ayhan S, Tuncer S, Erdogan D, Calguner E, Basterzï Y, Gozil R, Bahcelioglu M (2007) Effect of fresh and stored botulinum toxin a on muscle and nerve ultrastructure: an electron microscopic study. Ann Plast Surg 59(3):316–322
24. Gorgu M, Silistreli O, Karantinaci B, Ayhan M, Ozdemirkıran T, Celebisoy M (2006) Interaction of botulinum toxin type a with local anesthetic agents: an experimental study in rabbits. Aesth Plast Surg. 30:59–64
25. Capková K, Hixon MS, Pellett S, Barbieri JT, Johnson EA, Janda KD (2010) Benzylidenecyclopentenediones: first irreversible inhibitors against botulinum neurotoxin A's zinc endopeptidase. Bioorg Med Chem Lett 20(1):206–208
26. Vartanian AJ, Dayan SH (2005) Complications of botulinumtoxin A use in facial rejuvenation Facial Plast. Surg Clin North Am 13(1):1–10